Sensing and Bio-Sensing Research 11 (2016) 45–51

Contents lists available at ScienceDirect

Sensing and Bio-Sensing Research

journal homepage: www.elsevier.com/locate/sbsr

Monolayer MoS_2 and WSe_2 Double Gate Field Effect Transistor as Super Nernst pH sensor and Nanobiosensor

Abir Shadman *, Ehsanur Rahman, Quazi D.M. Khosru

Department of Electrical and Electronic Engineering, Bangladesh University of Engineering and Technology, Dhaka 1000, Bangladesh

ARTICLE INFO

Article history:
Received 27 June 2016
Received in revised form 24 August 2016
Accepted 26 August 2016

Keywords:
Double gate FET
2D material
pH sensor
Nernst limit
Drift diffusion
Nanobiosensor

ABSTRACT

Two-dimensional layered material is touted as a replacement of current Si technology because of its ultra-thin body and high mobility. Prominent transition metal dichalcogenides (TMD), Molybdenum disulphide (MoS_2), as a channel material for Field Effect Transistor has been used for sensing nano-biomolecules. Tungsten diselenide (WSe_2), widely used as channel for logic applications, has also shown better performance than other 2D materials in many cases. pH sensor is integrated with Nanobiosensor most often since charges (value and type) of many biomolecules depend on pH of the solution. Ion Sensitive Field Effect Transistor with Silicon and III–V materials has been traditionally used for pH sensing. Experimental result for MoS_2 field effect transistor as pH sensor has been reported in recent literature. However, no simulation-based study has been done for single layer TMD FET as pH sensor or bio sensor. In this paper, novel MoS_2 and WSe_2 monolayer double gate FETs are proposed for pH sensor operation in Super Nernst regime and protein detection. In case of pH sensing bottom gate operation ensures these monolayer FETs operating beyond Nernst limit of 59 mV/pH. Besides pH sensing, the proposed monolayer FETs also show reasonably high sensitivity in sub threshold region as protein detector. Simulation results found in this work reveal that, scaling of bottom gate oxide results in better sensitivity for both pH and biosensor while top oxide scaling exhibits an opposite trend in pH sensing.

1. Introduction

Ion-sensitive field-effect transistor (ISFET) is one of the most common approaches to label free nanobiosensor. Piet Bergveld first introduced ISFET in 1970. It is similar to the metal oxide semi-conductor field effect transistor (MOSFET). The ISFET, also known as pH sensor, has been used to measure ion's concentrations (H^+ or OH^-) in a solution. The two dimensional layered ISFET works in same principle as silicon based ISFETs. Protonation/deprotonation of the OH groups on the gate insulator (Fig. 1(a)) depending on the pH value of the electrolyte, changes the dielectric surface charge. It is the basic principal of pH detection. Lower pH value promotes the protonation of the solution, generating positive surface charges on the dielectric while higher pH value does the opposite. The resultant surface charge and the electrolyte voltage applied through a reference electrode also known as fluid/front gate voltage determine the surface potential. At a particular gate and drain bias in a FET, the change in pH would result in a change in surface charge in the oxide-electrolyte interface thereby changing the conductance of the channel material. This change in conductance will be reflected in the change in sensor current that would ultimately change the threshold voltage of the FET. This completes the basic operating principle of pH sensor. The pH sensitivity (mV/pH) for a conventional ISFET is defined by the changes of threshold voltage (V_T) at a given amount of pH changes. However, the pH sensitivity is always less than the well-known Nernst limit of 59 mV/pH for single gate operation. As reported in the literature [1,2], the limit in single-gated ISFET sensors can be breached by using the double gated field effect transistors. Most of the works until now of super-Nernst sensor involve silicon on insulator technology. In this work, we are proposing and studying monolayer TMD DGFET super-Nernst pH sensor for the first time. Because of highly scaled thickness up to an atomic plane and dangling bond free pristine surface [3,4], 2-D semiconducting transition metal dichalcogenides, such as MoS_2 and WSe_2, have been considered as prospective channel material for low power CMOS devices [5]. Monolayer MoS_2 and WSe_2 having considerable band gap (1.8 and 1.6 eV respectively [6]) results in higher I_{ON}/I_{OFF} ratio than the zero band gap graphene [7]. This property makes these materials suitable for low-power logic applications. Deblina Sarkar et al. [7] have recently demonstrated MoS_2 FET pH sensor. The work revealed that the lack of a band gap in graphene fundamentally limits sensitivity of graphene based sensor also. In this work the thickness of top and bottom gate oxides for both the TMD FETs have been varied from which it is found that increasing the thickness of top oxides results in reduced sensitivity while the trend is opposite for bottom oxide. This trend is also captured in the literature [1] for the Si FET. It is found that, with the simplifications presented in Section 2, inherent upper limit of pH sensitivity for these two TMD FET sensors is quite close to each other. This work has also investigated

* Corresponding author.
E-mail address: abir08@eee.buet.ac.bd (A. Shadman).

http://dx.doi.org/10.1016/j.sbsr.2016.08.005

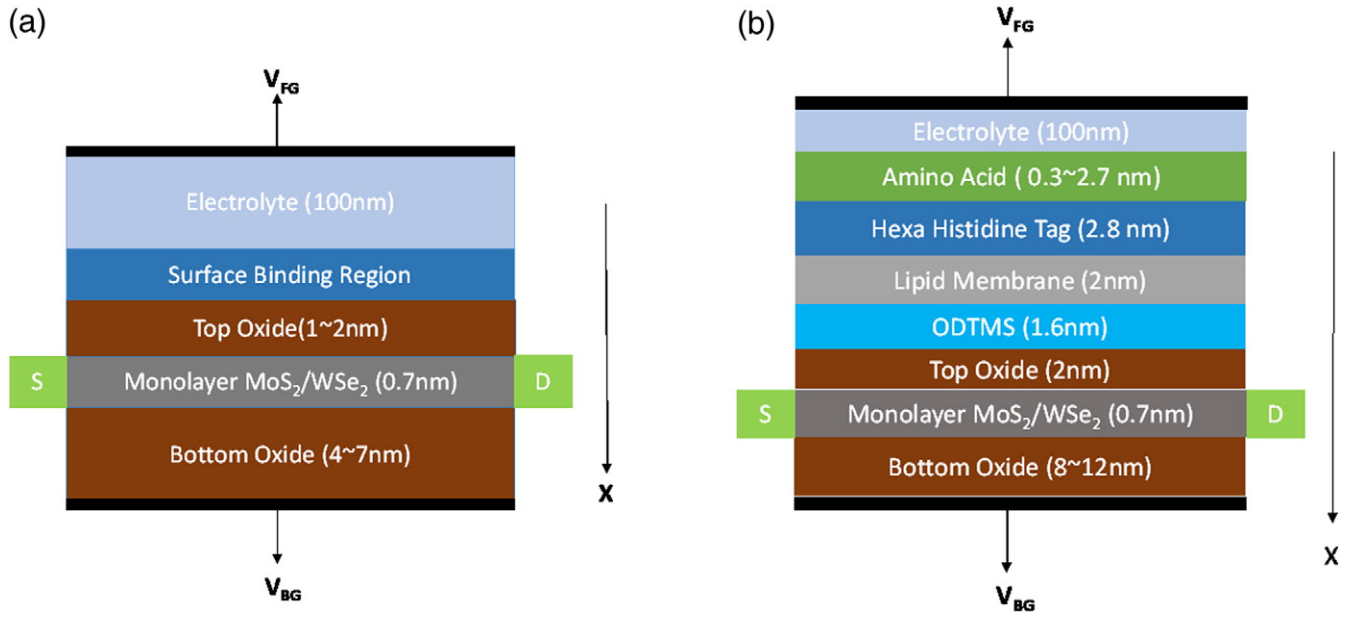

Fig. 1. (a) Simple Schematic representation of the pH sensor used in this work. (b) Simple Schematic structure of the biomolecule (amino acid) sensor used in this work. Here SiO_2 is used as top and bottom oxide for both pH and biosensor. None of the devices shown in this figure is drawn to scale.

a novel application of these materials in sensing biomolecules like protein. A comparative study of their sensitivity dependence on physical parameter like oxide thickness and device operation regime is carried out to maximize their detection capability in biosensor application. In this work we have developed a self-consistent Schrodinger Poisson solver which incorporates Boltzmann distribution in the electrolyte region to determine spatial charge and electrostatic potential distributions within the device for both pH and biomolecule sensor. In an attempt to provide more realistic prediction of the device physics simplification like Debye-Hückel approximation was avoided. The quantum mechanical charge density in the semiconductor was also taken into account.

2. Device structure & simulation methodology

Fig. 1(a) shows the schematic of the conventional double gate FET pH sensor used in this paper. Its channel material is single layer transitional metal dichalcogenide (monolayer MoS_2 and WSe_2). Transitional metal dichalcogenides are new type of materials that are being analyzed extensively as a prospective material to replace Si technology. Thickness of monolayer WSe_2 and MoS_2 has been considered 0.7 nm [8] and 0.65 nm [9] respectively in the literature. Although it is also common to treat the whole class of TMDC material with a thickness of 0.65 nm [10]. Gate dielectric is kept SiO_2 on both sides of the channel for this work. However, the simulation procedure [1] used in this work can easily take into account of various dielectrics. Here, fluid/front gate voltage, V_{FG} is kept 1 V for all simulations. In addition, Back gate voltage, V_{BG} is varied from 1 V to 5 V for operation over the Nernst limit. Top gate oxide is varied from 1 to 2 nm while the bottom gate oxide is varied from 4 to 7 nm. Single layer transition metal dichalcogenides' parameters have been taken from various references [11–15].

The electrolyte-top gate oxide interface is functionalized with surface groups (^{-}OH). Protons (H^+) in electrolyte react with these surface groups (-OH) which causes protonation and deprotonation. As a result of these reactions the net charge of -OH groups respond to the change of pH of the solution. The protonation/deprotonation of -OH groups are taken in to account by the surface binding model. According to the model, the chemical reactions occurring on the silicon oxide surface are as follows

$$\begin{aligned} SiOH + H_s^+ &\Longleftrightarrow SiOH_2^+ \\ SiO^- + H_s^+ &\Longleftrightarrow SiOH \end{aligned} \tag{1}$$

where H_s^+ represents the proton density near the surface region. The equilibrium constants for each of these reactions are described by the following equations:

$$\begin{aligned} \frac{[SiOH][H_s^+]}{[SiOH_2^+]} &= K_a \\ \frac{[SiO^-][H_s^+]}{[SiOH]} &= K_b \end{aligned} \tag{2}$$

The surface proton density H_s^+ is related to the bulk proton density H_B^+ at the solution by the Boltzmann distribution such that

$$\begin{aligned} [H_s^+] &= [H_B^+]\exp(-q\Phi_0/k_BT) \\ \Phi_0 &= \Phi_{x=0^+} - V_{FG} \end{aligned} \tag{3}$$

where Φ_0 is the electrostatic potential difference between the surface and the bulk electrolyte. The potential of the bulk electrolyte is fixed by the fluid gate (FG) bias. The bulk proton density $[H_B^+]$ is governed by pH of the electrolyte such that $pH = -\log_{10}[H_B^+]$. Now the net charge density of top oxide surface group can be expressed as

$$\sigma_{OH} = q\left([SiOH_2^+] - [SiO^-]\right) \tag{4}$$

In addition, the total density of the surface group is

$$N_s = [SiOH] + [SiOH_2^+] + [SiO^-] \tag{5}$$

Table 1
Equations used in this work [1].

Region	Equation
TMDC (channel)	$-\nabla\cdot(\epsilon_{2D}\nabla\Phi)=q(p-n+N_{imp})$ N_{imp} = impurity density
Top and bottom gate oxide	$-\nabla\cdot(\epsilon_{SiO_2}\nabla\Phi)=0$
Top oxide-electrolyte interface (Site binding region) (Only for pH sensor)	$(\epsilon_{SiO_2}\nabla\Phi_{at_{x=0-}})-(\epsilon_w\nabla\Phi_{at_{x=0+}})=Q_{OH}$ $\epsilon_w=80^*\epsilon_0$ $Q_{OH}=qN_s([OH_2^+]-[O^-])$ $N_s=5e14,(K_a,K_b)=(-2,6)$
ODTMS (only for biomolecule sensing)	$-\nabla\cdot(\epsilon_{ODTMS}\nabla\Phi)=0$
Lipid membrane (only for biomolecule sensing)	$-\nabla\cdot(\epsilon_{Lipid}\nabla\Phi)=Q_{Lipid}$ Q_{Lipid} = charge concentration due to lipid head group
Amino acid (only for biomolecule sensing)	$-\nabla\cdot(\epsilon_w\nabla\Phi)=\frac{2q^2Navo\ I_0}{K_BT}\sinh(\frac{q(\phi-V_{FG})}{K_BT})+qvNm$ v = amino acid charge per unit length Nm = amino acid density $Navo$ = Avogadro number.
Electrolyte	$-\nabla\cdot(\epsilon_w\nabla\Phi)=\frac{2q^2Navo\ I_0}{K_BT}\sinh(\frac{q(\phi-V_{FG})}{K_BT})$ $I_0=30$ mM $Navo=6.023\times10^{23}$

Now, Combining Eqs. (1)–(5), the expression of σ_{OH} as a function of the potential can expressed as

$$\sigma_{OH}=qN_s\frac{\left(10^{-pH}/10^{-pK_a}\right)e^{-\beta\Phi_0}-\left(10^{-pK_b}/10^{-pH}\right)e^{\beta\Phi_0}}{1+\left(10^{-pH}/10^{-pK_a}\right)e^{-\beta\Phi_0}-\left(10^{-pK_b}/10^{-pH}\right)e^{\beta\Phi_0}} \quad (6)$$

where $pK_a=-\log_{10}K_a$, $pK_b=-\log_{10}K_b$ and $\beta=q/k_BT$. pK_a and pK_b used in Eq. (6) define the surface group protonation/deprotonation affinity. In this work we use the well-known values of pK_a and pK_b for the SiO_2 available in the literature [16].

Thus, the boundary condition at the top oxide-electrolyte interface can be defined

$$(\varepsilon_{ox}\nabla\Phi_{x=0_-})-(\varepsilon_m\nabla\Phi_{x=0_+})=\sigma_{OH} \quad (7)$$

The device prototype for biosensor in Fig. 1(b) is consistent with recently reported biosensor [17]. However the distinct feature of this biosensor is that the conventional channel material Si is replaced by the monolayer MoS_2 and WSe_2 rather than the simple approach as used in recent literature [1]. The device used in this work is incorporated with proper surface functionalization to provide a more realistic conclusion. In this work as a model biomolecule we have used artificial protein structure (aspartic acid) where amino acids are tagged to a histidine chain. This artificial protein has an uncharged part since no amino acids are attached there. Since aspartic acids carries one negative charge each for binding to the tag, the rest of the histidine backbone is negatively charged. In this work, surface charge densities at the receptor site varies according to the charge of the aspartic acids. This change in surface charge will also cause a change in channel conductance. The electrolyte region includes the histidine-tagged aspartic acids as well as the neutral part of the tag. Thickness of top and bottom oxide is chosen appropriately to ensure a measurable change in device current with change in the number of aspartic acid. For the bio-functionalization of the semiconductor device, the top oxide layer is passivated by an ODTMS (octadecyltrimethoxysilane) monolayer. Dimension of various

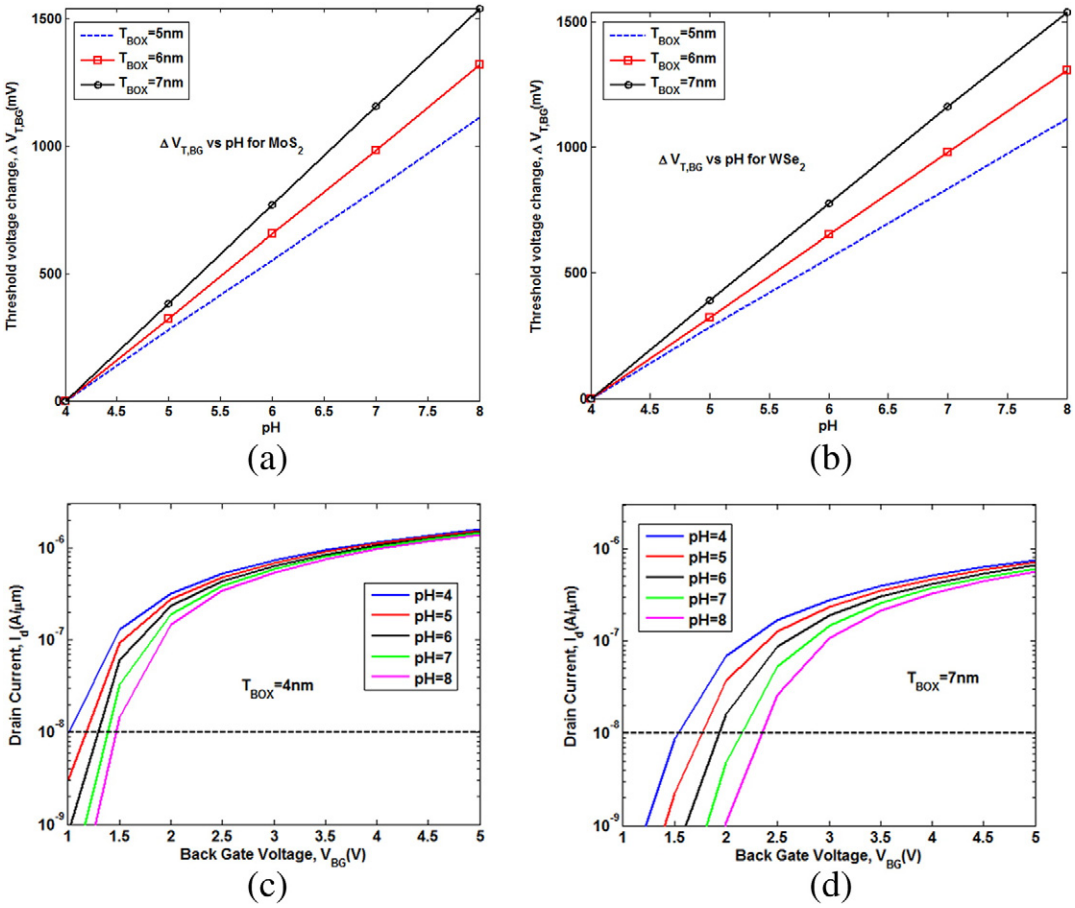

Fig. 2. (a)–(b) Show shift of V_T with pH for back gate operation which is above the Nernst limit and (c)(d) depict the differential increase of V_T for various pH with the increase of bottom oxide thickness. (c)–(d) provide insights towards the upward movement of the ΔV_T for various thicknesses and the linearity of the curves of (a)–(b) can be traced to the Eq. (8). (c)–(d) is for MoS_2.

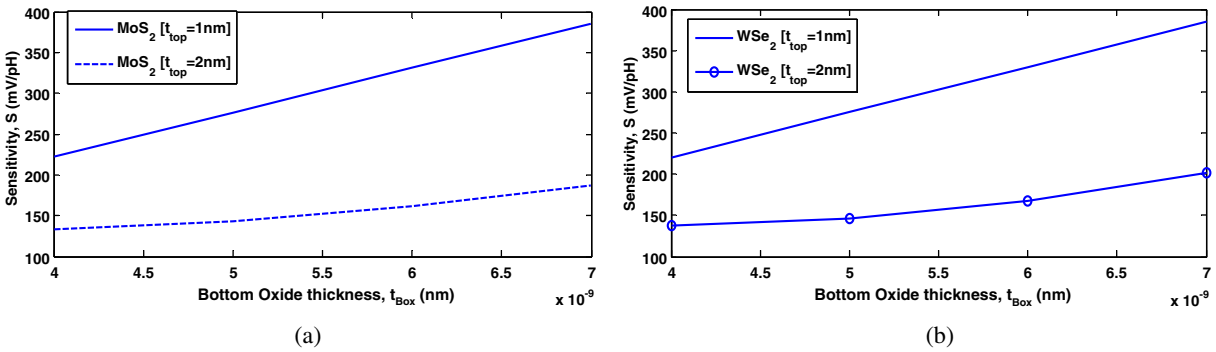

Fig. 3. (a)–(b) Depict the sensitivity of two TMD FET pH sensors for top oxide scaling.

surface functionalization layers like ODTMS, lipid membrane, and neutral part of histidine tag have been considered 1.6 nm, 2.0 nm and 2.8 nm respectively. Due to the functionalization by ODTMS no site-binding charge is present in top oxide electrolyte interface and therefore, no pH sensing is possible with this structure. Lipid membrane has been used as surface functionalization upon ODTMS layer which acts as receptor for the histidine tagged aspartic acid. For lipid membrane we have used similar material parameters like those of ODTMS. Since the lipid membrane layer is highly dense, no electrolyte is present within this layer. We have considered an electrolyte ion concentration of 30 mM. To consider human physiological condition the pH of the bulk electrolyte has been set to 7. Equations governing electrostatics in various regions have been listed in Table 1 for both pH and biosensor. Potential profile along the confinement direction obtained from the simulator used in this work is benchmarked with that of [1] (not shown). Drain bias is kept very small ($V_{ds} = 0.1$ V) which is typical for bio sensing application. We have used a long channel device with a length of 10 μm which allows us to use drift-diffusion equation for current in these monolayer sensors. We have used the current model in [5] which is specifically developed for monolayer TMDC devices. In current models to avoid complexity we have assumed Ohmic contacts and also ignore Interface traps.

3. Results and discussions as pH sensor

In this paper, we have varied top gate oxide and bottom gate oxide thickness for two different TMD FETs separately to find out how pH sensitivity changes with scaling and material parameter. In DGFET sensors, one sweeps the bottom gate (BG) bias, instead of fluid gate (FG), to obtain the transfer characteristics (I_d-V_{BG}) whereas a fixed bias is applied to the fluid gate, and the corresponding pH sensitivity is measured in terms of the threshold voltage shift. Due to asymmetry of top and bottom oxide thickness, the resultant asymmetry in top and bottom oxide capacitances originates the high pH sensitivity [2,13,18] of this sensor according to the following equation:

$$\frac{\Delta V_{BG}}{\Delta pH} = \alpha_{SN}\left(\frac{C_{tox}}{C_{box}}\right)\left(\frac{\Delta V_{FG}}{\Delta pH}\right) \tag{8}$$

Here in this work, we have used high gate bias for front gate ($V_{FG} = 1$ V). So, α_{SN} will be close to one [2,13,14] due to the operation in inversion regime. That is why back gate threshold voltage will vary approximately linearly with the change of pH considering that $\frac{\Delta V_{FG}}{\Delta pH}$ will be less than the Nernst limit and be almost constant during the sweep of back gate voltage.

3.1. Effect of various transition metal dichalcogenides as channel material

In this work, we have taken two widely used monolayer TMDs as channel material and the results are shown in the Fig. 2. From Fig. 2(a)–(b), two aspects are revealed. First, a very high almost identical sensitivity beyond Nernst limit is obtained for both dichalcogenides for a wide range of operation [pH 4 to 8] for various bottom oxide thicknesses. Second, sensitivity increases almost linearly with the increase of back oxide thickness while keeping top oxide thickness fixed at 1 nm. Here in defining sensitivity we have chosen V_T at pH = 4 as reference value. Fig. 2(c)–(d) supports the claim as evident from the extension of the spread of drain current in sub threshold region with the increase

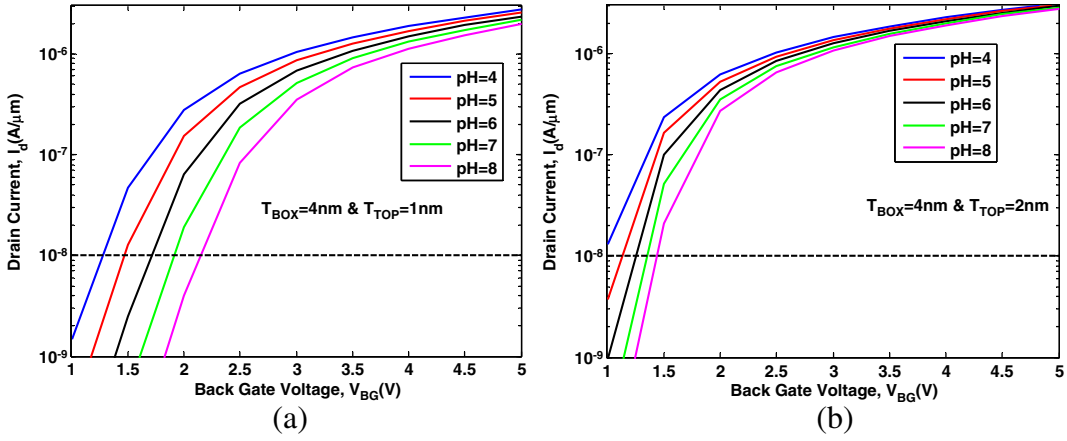

Fig. 4. (a)–(b) Shows the narrowing of drain current in the sub threshold region with the increase of top oxide thickness. This is for MoS_2.

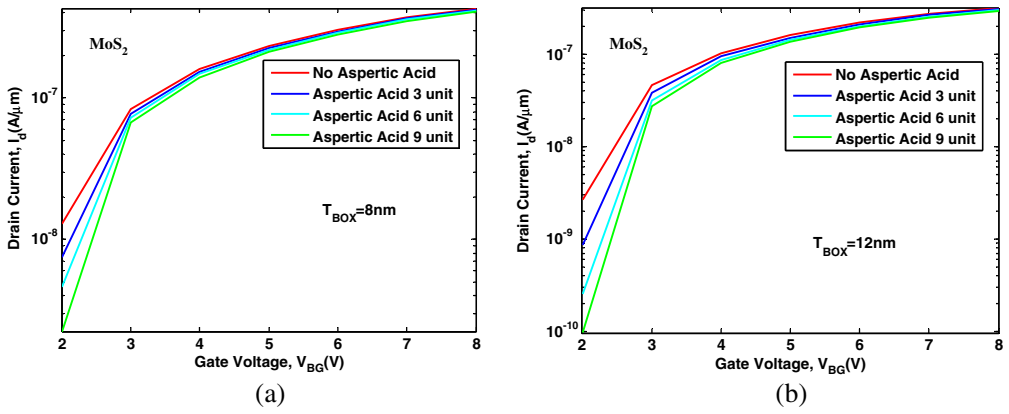

Fig. 5. (a), (b) $I_d - V_{BG}$ characteristics of MoS_2 monolayer biosensor for different no. of aspartic acids and for different bottom oxide thicknesses. Spread of the drain current in the subthreshold region gradually increases from $T_{BOX} = 8$ nm to $T_{BOX} = 12$ nm for various no. of aspartic acids. Change in current due to biomolecule is maximum in 'off' current regime whereas no significant difference in device current is observed for various aspartic acids in 'on' region.

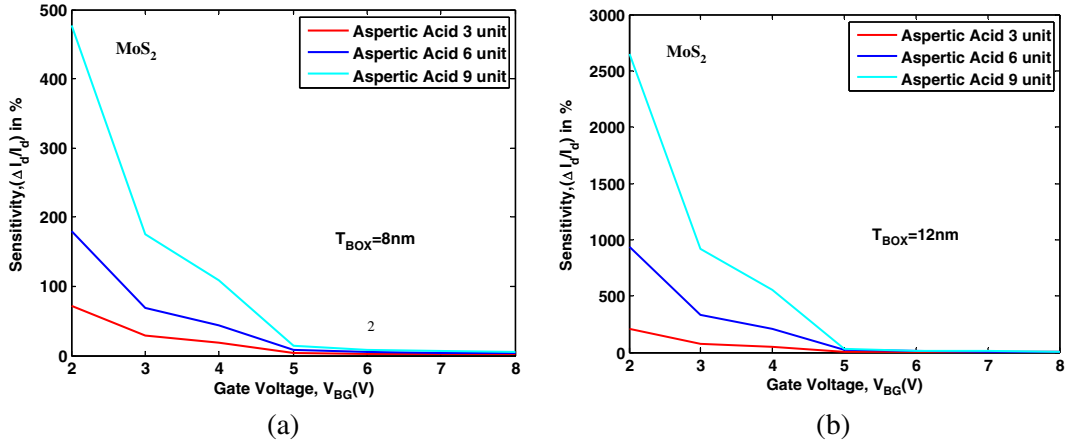

Fig. 6. (a), (b) Current sensitivity of MoS_2 monolayer biosensor for different no. of aspartic acids and for different bottom oxide thicknesses as a function of back gate voltage. Highest sensitivity is found in subthreshold region for all bottom oxide thickness. However, there is a notable increase in sensitivity in subthreshold regime with the increase in bottom oxide thickness for different no. of aspartic acids.

of back oxide thickness. This is also consistent with Eq. (8). Increase of T_{BOX} will reduce C_{box} and ultimately increases the sensitivity. However, it must be mentioned that the sensitivity reported in this work is an upper level estimation of yet to be experimentally measured sensitivity because of the assumptions made in Section 2. Almost identical sensitivity for two different dichalcogenides despite the dissimilarity of the

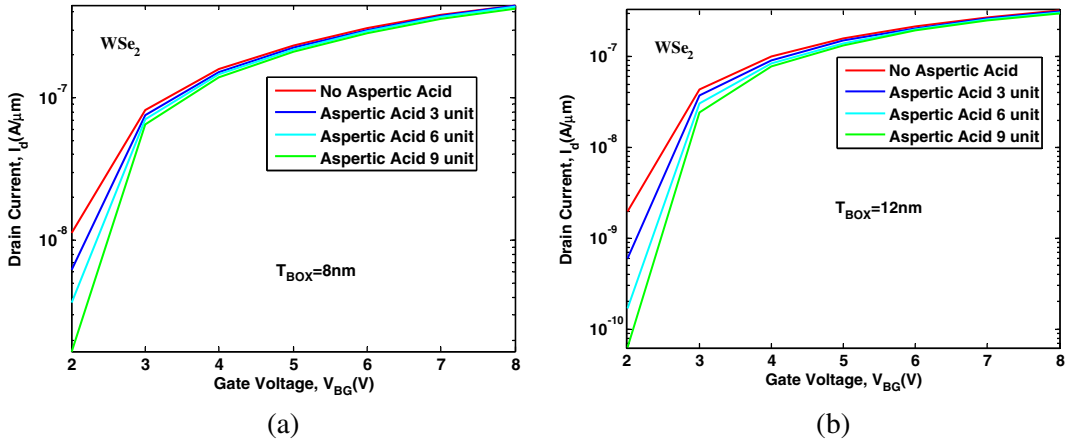

Fig. 7. (a), (b) $I_d - V_{BG}$ characteristics of WSe_2 monolayer biosensor for different no. of aspartic acids and for different bottom oxide thicknesses. Spread of the drain current in the subthreshold region gradually increases from $T_{BOX} = 8$ nm to $T_{BOX} = 12$ nm for various no. of aspartic acids. Change in current due to biomolecule is maximum in 'off' current regime whereas no significant difference in device current is observed for various aspartic acids in 'on' region.

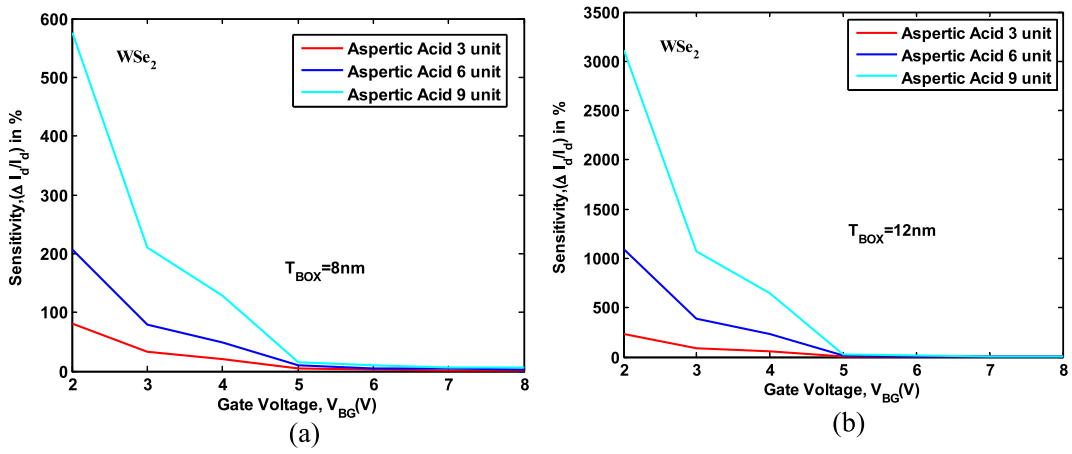

Fig. 8. (a), (b) Current sensitivity of WSe_2 monolayer biosensor for different no. of aspartic acids and for different bottom oxide thickness as a function of back gate voltage. Highest sensitivity is found in subthreshold region for all bottom oxide thickness. The sensitivity in subthreshold regime increases with the increase in bottom oxide thickness for different no. of aspartic acid.

material parameters can be attributed to the operation of the devices in inversion regime [18].

3.2. Effect of top oxide scaling

This subsection focuses on the simulation-based study showing the effect of scaling top oxide on sensitivity for two different TMD FET sensors. It is evident from the Eq. (8) and Fig. 3(a)–(b) that increasing the top oxide thickness results in a reduction of sensitivity. This finding is consistent with the trend found in recent literature [1]. Fig. 4(a)–(b) shows the narrowing of the spread of drain current in sub threshold region with the increase of top oxide thickness. This causes the decrease of sensitivity. Almost identical sensitivity has been found for both TMD FET sensors suggesting each TMD as a viable channel material for Super Nernst pH sensing.

4. Result and discussions as nanobiosensor

To evaluate the prospect of MoS_2 and WSe_2 monolayer materials in a FET based nanobiosensor, we have considered more realistic structure of Fig. 1(b) than simple description presented in [1]. We have varied the no. of aspartic acid charges to find out the sensitivity of these sensors. Sensitivity in the case of biosensor is defined as the ratio of the difference in current before and after biomolecule binding to the lower of the two currents [19]. Therefore, sensitivity is unit less for biosensor unlike pH sensor. The magnitude of the negative protein charge density increases with the number of aspartic acids.

This results in a potential decrease in the charged part of the protein region. As a result, surface potential (potential at top gate oxide-receptor interface) decreases with increasing protein charge. This potential acts as top gate voltage in current simulator. Since surface potential is decreasing with the increasing no. of aspartic acid, current will also decrease for all monolayer FETs as seen from Figs. 5 and 7.

As seen from the Figs. 6 and 8, the relative change in transistor 'on' current with the increasing no. of aspartic acid is relatively small compared to that in subthreshold regime. This is due to the fact that in 'on' condition current is already set to a high value, so a small change in surface potential due to the attachment of a biomolecule results in a corresponding small change in the drain current which is not so significant. However, in completely off device or in subthreshold regime, FET conducts little or no current. Therefore, a small change in surface potential due to binding of protein causes relatively larger change in drain current. This phenomenon can be explained from another viewpoint. Drain current-gate voltage relationship is exponential, quadratic and linear in subthreshold, saturation and triode regions respectively; hence, the sensitivity in the subthreshold region is much higher compared to those in the saturation and linear regions. These findings indicate that biosensor operation in subthreshold regime will optimize the sensor response for these monolayer FETs while simultaneously improving the lower limit of bio molecule detection. Another point to note from Figs. 6 and 8 is that for both monolayer material FET sensors sensitivity increases with bottom oxide thickness. This trend in sensitivity seems reasonable since as we increase the bottom oxide thickness, the control of bottom gate voltage on channel conductivity weakens. Hence, effect of biomolecule charge on channel conductivity tends to be more dominant for higher bottom oxide thickness which might explain such increase in sensitivity.

5. Conclusion

In this work, two widely used monolayer transition metal dichalcogenides based double gate FETs have been proposed as pH and biosensor. These two dissimilar FETs have demonstrated almost similar intrinsic upper level of sensitivity. The proposed pH sensors have shown excellent pH sensitivity while beating the Nernst limit. Such high sensitivity can be attributed to back gate operation and the sensitivity of these FETs increases with back oxide thickness while decreasing with top oxide thickness. This trend is quite similar to that of experimentally reported Silicon FET. These two TMD FETs should be promising candidates for Super Nernst pH sensing in future, as the growth techniques of 2D material FETs continue to flourish. These materials are also viable options in implementing FET based biosensor because of their high sensitivities especially in the subthreshold regime with properly sized top and bottom oxide. Application of these FETs as biosensor can be further extended to the detection of other biomolecules like DNA, Biotin and Streptavidin etc.

References

[1] J. Go, P.R. Nair, B. Reddy, B. Dorvel, R. Bashir, M.A. Alam, Beating the Nernst limit of 59 mV/pH with double-gated nano-scale field-effect transistors and its applications to ultra-sensitive DNA biosensors, Tech. Dig.-Int. Electron Devices Meet. IEDM, 2, 2010, pp. 202–205.
[2] M.J. Spijkman, J.J. Brondijk, T.C.T. Geuns, E.C.P. Smits, T. Cramer, F. Zerbetto, P. Stoliar, F. Biscarini, P.W.M. Blom, D.M. De Leeuw, Dual-gate organic field-effect transistors as potentiometrie sensors in aqueous solution, Adv. Funct. Mater. 20 (6) (2010) 898–905.
[3] W. Cao, J. Kang, S. Bertolazzi, A. Kis, K. Banerjee, Can 2D-nanocrystals extend the lifetime of floating-gate transistor based nonvolatile memory? IEEE Trans. Electron Devices 61 (10) (2014) 3456–3464.
[4] W. Cao, J. Kang, W. Liu, Y. Khatami, D. Sarkar, K. Banerjee, 2D electronics: graphene and beyond, European Solid-state Device Research Conference 2013, pp. 37–44.

[5] W. Cao, J. Kang, W. Liu, K. Banerjee, A compact current-voltage model for 2D semiconductor based field-effect transistors considering interface traps, mobility degradation, and inefficient doping effect, IEEE Trans. Electron Devices 61 (12) (2014) 4282–4290.
[6] K.S. Novoselov, A.K. Geim, S.V. Morozov, D. Jiang, Y. Zhang, S.V. Dubonos, I.V. Grigorieva, A.A. Firsov, Electric field effect in atomically thin carbon films, Science 306 (5696) (2004) 666–669 (80-.).
[7] D. Sarkar, W. Liu, X. Xie, A.C. Anselmo, S. Mitragotri, K. Banerjee, MoS_2 field-effect transistor for next-generation biosensors, ACS Nano 8 (4) (2014) 3992–4003.
[8] H. Fang, S. Chuang, T.C. Chang, K. Takei, T. Takahashi, A. Javey, High-performance single layered WSe_2 p-FETs with chemically doped contacts, Nano Lett. 12 (7) (2012) 3788–3792.
[9] Y. Yoon, K. Ganapathi, S. Salahuddin, How good can monolayer MoS_2 transistors be? Nano Lett. 11 (9) (2011) 3768–3773.
[10] W. You, P. Su, A Compact Subthreshold Model for Short-channel Monolayer Transition Metal Dichalcogenide Field-effect Transistors, vol. 63, no. 7, 2016 2971–2974.
[11] R.K. Ghosh, S. Mahapatra, S. Member, Monolayer transition metal dichalcogenide, IEEE J. Electron Devices Soc. 1 (10) (2013) 175–180.
[12] C. Gong, H. Zhang, W. Wang, L. Colombo, R.M. Wallace, K. Cho, Band alignment of two-dimensional transition metal dichalcogenides: application in tunnel field effect transistors, Appl. Phys. Lett. 103 (5) (2013) 0–4.
[13] J. Chang, L.F. Register, S.K. Banerjee, Comparison of ballistic transport characteristics of monolayer transition metal dichalcogenides (TMDs) MX_2 (M = Mo, W; X = S, Se, Te) n-MOSFETs, Int. Conf. Simul. Semicond. Process. Devices, SISPAD, 2, 2013, pp. 408–411.
[14] S.U.Z. Khan, Q.D.M. Khosru, Quantum mechanical electrostatics and transport simulation and performance evaluation of short channel monolayer WSe_2 field effect transistor, ECS Trans. 66 (14) (2015) 245–254.
[15] K. Banerjee, W. Liu, J. Kang, High-performance field-effect-transistors on monolayer-WSe_2, Transactions, E C S Society, The Electrochemical, 58, no. 7, 2013, p. 2182.
[16] D. Landheer, G. Aers, W.R. McKinnon, M.J. Deen, J.C. Ranuarez, Model for the field effect from layers of biological macromolecules on the gates of metal-oxide-semiconductor transistors, J. Appl. Phys. 98 (4) (2005).
[17] S. Birner, C. Uhl, M. Bayer, P. Vogl, Theoretical model for the detection of charged proteins with a silicon-on-insulator sensor, J. Phys. Conf. Ser. 107 (2008) 012002.
[18] J. Go, P.R. Nair, M.A. Alam, Theory of signal and noise in double-gated nanoscale electronic pH sensors, J. Appl. Phys. 112 (3) (2012).
[19] D. Sarkar, W. Liu, X. Xie, A.C. Anselmo, S. Mitragotri, K. Banerjee, MoS_2 field-effect transistor for next-generation label-free biosensors, ACS Nano 8 (4) (2014) 3992–4003.